Wrapping dynamics and critical conditions for active nonspherical nanoparticle uptake

Ke Xiao*
Wenzhou Institute, University of Chinese Academy of Sciences, Wenzhou 325016, People's Republic of China and Department of Physics, College of Physical Science and Technology, Xiamen University, Xiamen 361005, People's Republic of China

Rui Ma and Chen-Xu Wu†
Fujian Provincial Key Lab for Soft Functional Materials Research, Research Institute for Biomimetics and Soft Matter, Department of Physics, College of Physical Science and Technology, Xiamen University, Xiamen 361005, People's Republic of China

(Received 15 January 2023; revised 26 March 2023; accepted 17 April 2023; published 1 May 2023)

The cellular uptake of self-propelled nonspherical nanoparticles (NPs) or viruses by cell membrane is crucial in many biological processes, but its universal dynamics have yet to be elucidated. In this study, using the Onsager variational principle, we obtain a general wrapping equation for nonspherical self-propelled nanoparticles. Two analytical critical conditions are theoretically found, indicating a continuous full uptake for prolate particles and a snapthrough full uptake for oblate particles. They precisely capture the full uptake critical boundaries in the phase diagrams numerically constructed in terms of active force, aspect ratio, adhesion energy density, and membrane tension. It is found that enhancing activity (active force), reducing effective dynamic viscosity, increasing adhesion energy density, and decreasing membrane tension can significantly improve the wrapping efficiency of the self-propelled nonspherical nanoparticles. These results give a panoramic view of the uptake dynamics of active nonspherical nanoparticles, and may offer instructions for designing an effective active NP-based vehicle for controlled drug delivery.

DOI: 10.1103/PhysRevE.107.054401

I. INTRODUCTION

The lipid bilayer plasma membrane, a physical barrier defining organelles of cells and plenty of their surrounding environment, plays a crucial role for a spectrum of biological processes [1]. Examples range from the transduction of biochemical signals and the intake of nutrients [2] to budding and fission [3,4], and endocytosis of viruses, pathogens, and particles [5,6]. The engulfing of a particle or virus (pathogen) by a plasma membrane is a widely encountered phenomenon in endocytosis processes, including inter- and intracellular transport [7], delivering therapeutic agents enveloped by nanoparticles (NPs) into tumor cells [8–10] and virus infection [11–13]. Especially, cellular uptake, which involves the interaction between cell membrane and NPs or viruses, is an essential step for a wide range of healthy and disease-related processes [12].

Over the past two decades, considerable efforts using experiment, theoretical modeling, and numerical simulation have been devoted to characterizing how the physical parameters, including particle size [14–20], shape [21–23], elastic properties of invading particles [24–28], ligand and receptor density [29–31], as well as the mechanical properties of the membrane [32,33], affect the invading behaviors. Though the cellular uptake of passive particles via endocytic process has been studied extensively, little work has been done on the active entry of self-propelled bacterial pathogens. To name a few examples, it has been found that some cytosolic bacteria such as *Rickettsia rickettsii* are able to produce active force to facilitate their mobility by forming actin tails [34], and *Listeria monocytogenes* can generate active force to push out a tube-like protuberance from the plasma membrane by hijacking the actin polymerization-depolymerization apparatus of their host [35–39]. How the active force of these self-propelled agents affects the engulfing dynamics at the cell membrane remains to be elucidated.

Recently, many model systems using lipid vesicles to encapsulate natural swimmers (*Escherichia coli* bacteria, *Bacillus subtilis* bacteria, etc.) or artificial microswimmers (synthetic Janus particles) have been developed to study the active membrane behaviors in vitro [40–45]. Such systems are out of equilibrium and hence give rise to many intriguing behaviors, such as membrane fluctuations and large deformations [40,41], shape transformations [42–44], and even deformation of lipid vesicles into flagellated swimmers [45]. Therefore, the specific interactions between vesicles and bacteria or artificial self-propelled particles plays a key role in designing active matter systems [46]. In the limit of low membrane tension and weak reversible adhesion, Spanke *et al.* [47] experimentally investigated how the spontaneous wrapping dynamics of micron-sized particles by giant unilamellar vesicles changes with the adhesion energy. By combining computer simulations and theoretical analysis, the cellular uptake of active particles in the absence of membrane ten-

*xiaoke@ucas.ac.cn
†cxwu@xmu.edu.cn

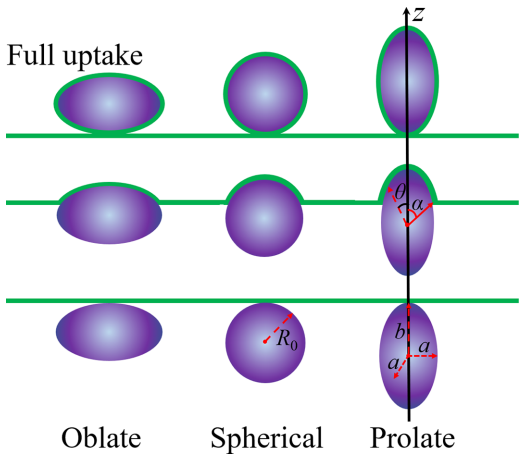

FIG. 1. Schematic depicting wrapping phases of an active particle from nonwrapping to partial wrapping and to full uptake.

sion was studied [48], and the deterministic and stochastic uptake dynamics of passive NPs with different geometries were also reported [21]. Understanding such effects of forces and membrane properties (adhesion energy density and membrane tension) on the dynamics of cellular uptake is critical to designing efficient strategies for potential biomedical applications, including drug and gene delivery [49–51], cell operation and manipulation [52,53], and bioimaging and sensing [8,54]. However, in reality, as many pathogens and viruses are nonspherical [55], such as egg-shaped *malaria parasite* [56] and cylindrical *Listeria monocytogenes*, a detailed and comprehensive investigation of how the uptake time depends on the active force, the particle's aspect ratio, the viscosity, and the membrane properties (adhesion energy density and membrane tension) is needed.

II. THEORETICAL MODELING

We consider a fluidic membrane invaded by an active self-propelled nanoparticle modeled as an axis-symmetric ellipsoid (prolate or oblate spheroid). For simplicity, the particle is assumed to be symmetrically aligned with the membrane initially under a constant active force in the z direction, as shown in Fig. 1, where a and b denote the semiaxes perpendicular to and along the principle rotational axis, respectively. The geometry of the particle is parametrized by an aspect ratio $e = b/a$, with $e > 1$ for a prolate ellipsoid and $e < 1$ for an oblate one. It should be noted that passive particles may undergo orientational rotation, possibly due to stochastic thermal fluctuation of the membrane [57]. Following the classical Canham-Helfrich continuum model [16,58,59], the total free energy of such a system is given by

$$E_{\rm tot} = \int_{A_{\rm mem}} \frac{\kappa}{2}(2H)^2 dA + \sigma \Delta A - \int_{A_{\rm ad}} \omega\, dA - fZ, \qquad (1)$$

where the elastic energy of the membrane, the adhesion energy between the particle and the membrane, and the work done by the active particle are taken into account. Here we neglect the contribution made by the membrane part detached from the particle. In practice, it is convenient to write the area element in terms of polar angle: $dA = 2\pi a^2 \sin\theta\sqrt{\cos^2\theta + e^2\sin^2\theta}\,d\theta$. The first term of Eq. (1), with κ the bending rigidity and H the local mean curvature, denotes the bending energy of the membrane

$$E_{\rm bend} = \int_0^{\alpha} \pi\kappa e^2 \sin\theta \frac{[2+(e^2-1)\sin^2\theta]^2}{[1+(e^2-1)\sin^2\theta]^3} \times \sqrt{\cos^2\theta + e^2\sin^2\theta}\,d\theta, \qquad (2)$$

an integral over the contact area between the membrane and the particle (see the detailed derivation in the Appendix). For simplicity, the contribution made by the elastic energy of the free membrane part detached from the particle is neglected [2,21]. The second term of Eq. (1) is an energy

$$E_{\rm ten} = \int_0^{\alpha} 2\pi\sigma a^2 \sin\theta \left[1 - \frac{\cos\theta}{\sqrt{\cos^2\theta + e^2\sin^2\theta}}\right] \times \sqrt{\cos^2\theta + e^2\sin^2\theta}\,d\theta, \qquad (3)$$

contributed by membrane tension σ (see the detailed derivation in the Appendix). The third term of Eq. (1) represents the gain in adhesive energy, which is characterized by a negative adhesive energy $-\omega$ per unit area. Typically, the interaction between membranes and particles can be classified as nonspecific adhesion and specific adhesion, among which the nonspecific adhesion of NPs to cell membranes refers to the physical attachment of the NPs to the cell membranes without involving specific receptor-ligand interactions. The specific membrane-NP adhesion (i.e., receptor-mediated endocytosis) refers to the specific binding of receptor and ligand molecules that are anchored in the membrane and to the particle surface. In this paper, we only consider the case of the nonspecific interaction between the cell membrane and nanoparticle. The last term of Eq. (1) arises from work done by an active force f acting on the particle, which can be calculated as $E_{\rm f} = -fae(1-\cos\alpha)$.

It has been found that as the particle is being engulfed by the membrane, it is the friction force near the membrane-particle contact line with its circumference given by $L(\alpha) = 2\pi a\sin\alpha$ that largely dissipates the energy [47]. In the limit of low Reynolds number, the dissipation function reads (see the detailed derivation in the Appendix)

$$\Phi = \pi\eta a^3 \sin\alpha(\cos^2\theta + e^2\sin^2\theta)\dot{\alpha}^2, \qquad (4)$$

where η is the effective dynamic viscosity with a typical order of 1 Pa s. In order to obtain the equation governing the wrapping dynamics of the active particle, following the Onsager variational principle [60,61] we construct a Rayleighian $\mathcal{R} = \dot{E}_{\rm tot} + \Phi$, with $\dot{E}_{\rm tot}$ the time derivative of the total free energy

$$\dot{E}_{\rm tot} = \left\{\frac{\kappa e^2}{a^2}\frac{[2+(e^2-1)\sin^2\alpha]^2}{[1+(e^2-1)\sin^2\alpha]^3} + \times 2\sigma\left(1 - \frac{\cos\alpha}{\sqrt{\cos^2\alpha + e^2\sin^2\alpha}}\right) - 2\omega\right\} \times \pi a^2 \sin\alpha\sqrt{\cos^2\alpha + e^2\sin^2\alpha}\,\dot{\alpha} - fae\sin\alpha\dot{\alpha}, \qquad (5)$$

and Φ the energy dissipation function. Minimizing $\mathcal{R}$ with respect to $\dot{\alpha}$ following the Onsager variational principle, i.e.,

TABLE I. Parameters used in the numerical calculations.

Parameters	Used value	References
Membrane bending rigidity	$\kappa = 25\,k_BT$	[62,63]
Membrane tension	$\sigma = 0.9 \times 10^{-5}$ N/m	[21,62]
Adhesion energy per area	$\omega = 0.044$ mJ/m^2	[21,62]
Effective dynamic viscosity	$\eta = 1$ Pa s	[2,19]

$\partial\mathcal{R}/\partial\dot{\alpha} = 0$, we obtain the cellular uptake dynamics equation

$$\dot{\alpha} = \frac{1}{\eta a\sqrt{\cos^2\alpha + e^2\sin^2\alpha}}\left\{\omega + \frac{fe}{2\pi a\sqrt{\cos^2\alpha + e^2\sin^2\alpha}} - \frac{\kappa e^2}{2a^2}\frac{[2+(e^2-1)\sin^2\alpha]^2}{[1+(e^2-1)\sin^2\alpha]^3} - \sigma\left(1 - \frac{\cos\alpha}{\sqrt{\cos^2\alpha + e^2\sin^2\alpha}}\right)\right\} \tag{6}$$

for a nonspherical active particle. For spherical particles $a = b = R$, the above equation reduces to Eq. (2) in Ref. [21] if $f = 0$.

A detailed theoretical analysis of Eq. (6) shows that there exist two types of critical conditions for a full uptake to occur. One is governed by $\dot{\alpha}|_{\alpha=\pi} = 0$, or

$$\omega + \frac{f}{2\pi a}e - \frac{2\kappa}{a^2}e^2 - 2\sigma = 0, \tag{7}$$

corresponding to a second-order wrapping transition for prolate particles and spherical particles, which, in particular, own a critical radius $R_c = [-f + \sqrt{f^2 + 32\pi^2\kappa(\omega - 2\sigma)}]/[4\pi(\omega - 2\sigma)]$ when $\omega \neq 2\sigma$. It is found from Eq. (6) that during the dynamic process, the wrapping angle for oblate particles experiences a plateau near $\pi/2$. By considering a small variation $\Delta\alpha$ from $\pi/2$ and performing a Taylor expansion for the right side of Eq. (6), we have the other critical condition

$$\omega + \frac{f}{2\pi a} - \frac{\kappa(1+e^2)^2}{2a^2e^4} - \sigma - \frac{B^2}{4C} = 0 \tag{8}$$

for a first-order wrapping transition from a no- or partial wrapping to a full uptake. This is obtained by using $\dot{\alpha}|_{\alpha=\pi/2+B/(2C)} = 0$ with $B = \sigma/e$ and

$$C = \frac{1-e^2}{2e^2}\left(\sigma - \omega - \frac{f}{\pi a}\right) + \frac{\kappa(3e^2+7)}{4a^2e^6}.$$

Here, $-B$ and C correspond to the coefficients of $\Delta\alpha$ and $\Delta\alpha^2$ terms of the Taylor expansion of Eq. (6), respectively. If the membrane tension satisfies $(2e^2-1)\sigma \ll \kappa(3e^2+7)/(a^2e^4) - 2(1-e^2)[\omega + f/(\pi a)]$, then the last term can be discarded and the above condition reduces to

$$\omega + \frac{f}{2\pi a} - \frac{\kappa(1+e^2)^2}{2a^2e^4} - \sigma = 0. \tag{9}$$

Eqations (7) and (8) equivalently represent force-balance conditions among the four types of forces corresponding to the four terms in Eq. (1), with the active force and the adhesion balancing against the elastic force and the membrane tension.

III. RESULTS AND DISCUSSION

In order to investigate the wrapping dynamics of a nonspherical active particle, we first solve Eq. (6) numerically. In this paper, the used parameter values, if not varied, are summarized in Table I. For an oblate spheroid, the engulfing angle (black curves) as shown in Fig. 2(a) exhibits a plateau around $\alpha = \pi/2$, followed by a rapid increase of wrapping angle, indicating that there exists an accelerating uptake at this point. The low wrapping velocity (blue curve) at the plateau comes from the sharp increase of bending energy due to the high curvature, which hinders the wrapping process in this region. Here, the wrapping velocity is defined as the derivative of wrapping angle with respect to time. In contrast, the prolate spheroid and the spherical particle show a similar wrapping behavior, as shown in Figs. 2(b) and 2(c). The wrapping velocity for the spherical particle shows a significant and monotonic drop-off and slows down to a fully wrapping state after the particle is initially internalized. For the prolate spheroid, the engulfing velocity increases at the beginning, followed by a dramatic decrease, levels of,f and finally terminates at a full uptake ($\alpha/\pi = 1$) [Fig. 2(c)]. As the elastic energy of the membrane is the integral of curvature over the contact area, which is small at the beginning for the prolate spheroid, the contribution made by elasticity as an obstructor of wrapping is trivial and that is the reason why the engulfing velocity increases.

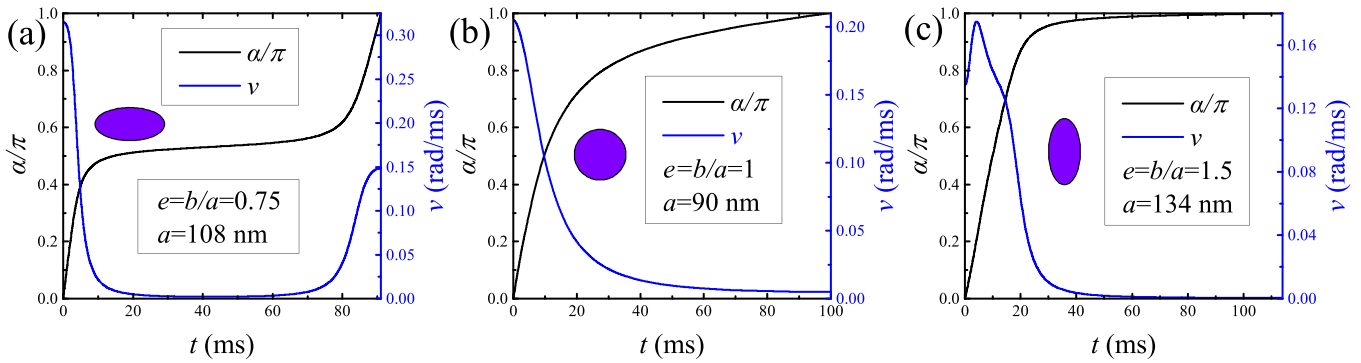

FIG. 2. The engulfing angle α/π and the wrapping velocity v of a particle with different aspect ratios (a) $e = 0.75$, (b) $e = 1$, and (c) $e = 1.5$. Notice that the particle volume is not fixed in this figure.

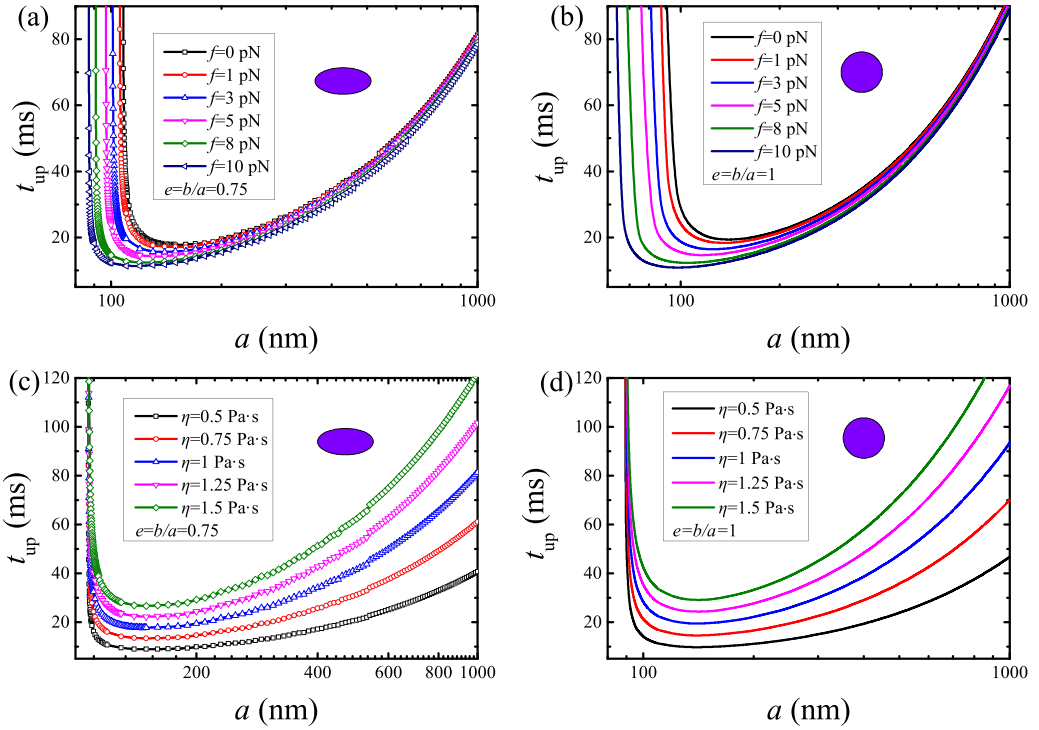

FIG. 3. Uptake time as a function of particle size for (a) oblate particle and (b) spherical particle with different active forces, and for (c) oblate particle and (d) spherical particle with different effective dynamic viscosities. The aspect ratio for oblate particles is kept unchanged.

Figure 3 shows how the uptake time depends on the particle size for different active forces and dynamic viscosities. Given f [Figs. 3(a) and 3(b)] or η [Figs. 3(c) and 3(d)], all the uptake times share a similar feature that with the increase of particle size, t_{up} drops very quickly before it bounces back mildly. Such a similarity of wrapping behavior indicates that there exists a common critical condition related to force, viscosity, and particle size for them beyond which a full uptake occurs. The calculation results also demonstrate that particles with larger active forces are taken up faster than those with smaller forces, showing that particle activity facilitates the uptake process. This conclusion is in line with the simulation prediction in Ref. [48] that the uptake efficiency can be enhanced with the increase of Péclet, a quantity measuring the strength of active force. The dynamic viscosity also affects the wrapping dynamics. It is found, as shown in Figs. 3(c) and 3(d), that decreasing the effective dynamic viscosity η clearly decreases the uptake time for the occurrence of the complete uptake. A large viscosity inhibits the uptake process and hence leads to longer uptake time. To achieve a faster (slower) wrapping process, enhancing (weakening) the particle activity and reducing (raising) the effective dynamic viscosity might be an effective option.

Pathogens and viruses come in many different shapes [55], so it is necessary to study the dynamic wrapping behaviors of nonspherical particles by membranes. Here we focus our discussion on the ellipsoid with its shape characterized by aspect ratio through an f-e phase diagram constructed for

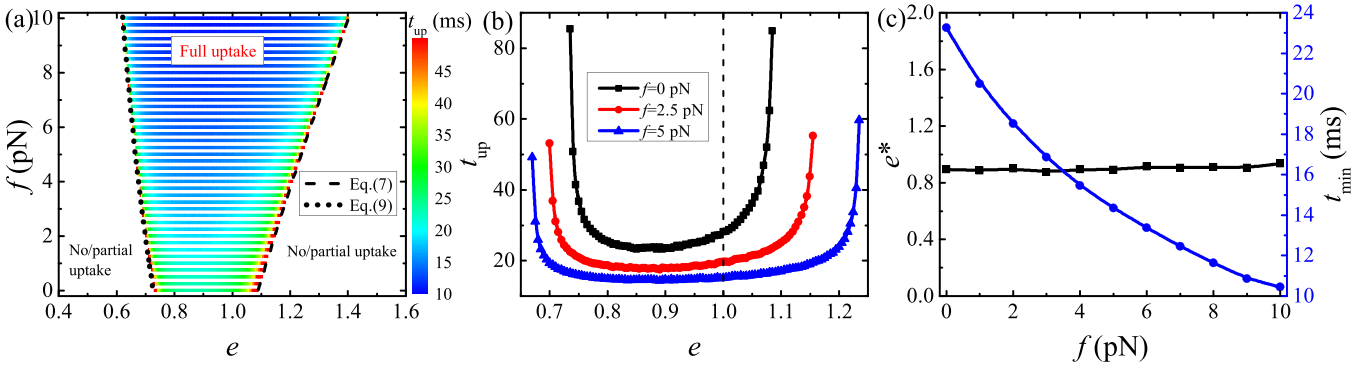

FIG. 4. (a) An f-e phase diagram characterizes the effects of the active force and the particle aspect ratio (fixed volume) on the uptake time. (b) The uptake time shows a nonmonotonic dependence for oblate particles and a monotonic one for prolate particles. (c) The activity of particles decreases the uptake time considerably but not the optimum aspect ratio.

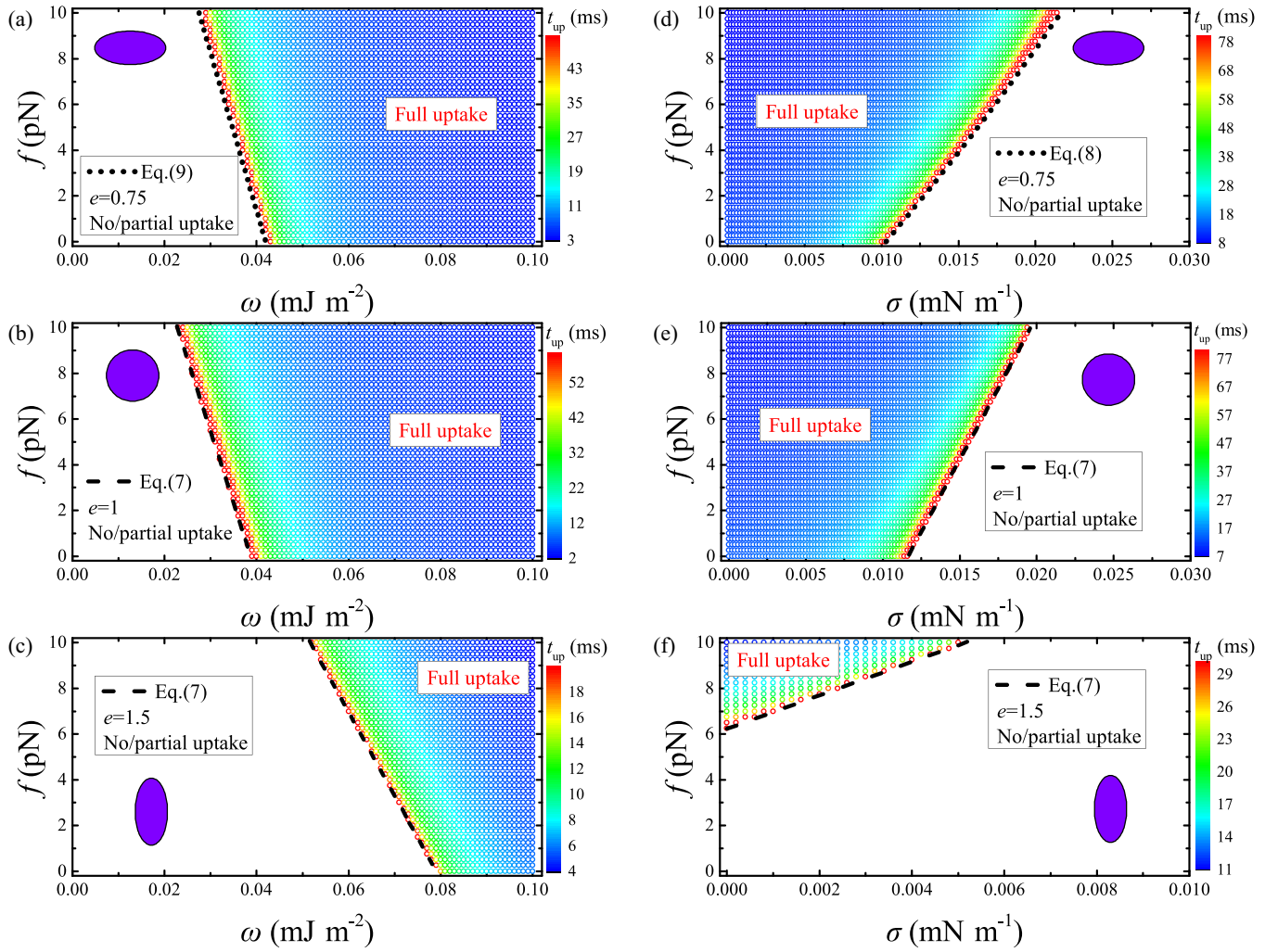

FIG. 5. Wrapping time t_{up} as a function of f and ω for (a) oblate ellipsoidal, (b) spherical, and (c) prolate ellipsoidal particles at equal particle volume. Uptake times as a function of active force f and membrane tension σ for (d) oblate ellipsoidal, (e) spherical, and (f) prolate ellipsoidal particles with fixed particle volume.

the uptake time under the condition of fixed particle volume ($V = 4\pi ea^3/3 = 4\pi R_0^3/3$ with $R_0 = 100\,\mathrm{nm}$), as shown in Fig. 4. It is found that a prolate ellipsoidal particle is taken up slower than a spherical one, while upon decreasing the aspect ratio, the uptake time for the active oblate ellipsoidal particles displays a nonmonotonic feature, in stark contrast to the monotonic dependence for active prolate particles, as shown in Figs. 4(a) and 4(b). In order to investigate the minimum uptake time and its corresponding optimum aspect ratio, we plot Fig. 4(c), which verifies that enhancing the activity gives rise to the wrapping efficiency (with a decrease of t_{up}), but does not effect the optimum aspect ratio much. Besides, the two analytical critical curves based on Eqs. (7) and (9) precisely fall onto the two boundaries separating the full uptake and the no- or partial uptake regimes, indicating once again that there exist two ways for a nonspherical particle to reach full wrapping, i.e., a continuous uptake for prolate particles and a snapthrough uptake for oblate particles. Such a conclusion is in agreement with the simulations done by Khosravanizadeh *et al.* [64] that oblate particles exhibit a discontinuous wrapping phase transition from partial wrapping to full wrapping during the uptake process, while prolate particles show a continuous one.

To gain more insight into the effects of the membrane properties on the uptake time, we explore the wrapping dynamics of active particles with different adhesion energy densities and membrane tensions. The colored contour maps of t_{up} on the f-ω [see Figs. 5(a)–5(c)] and f-σ [see Figs. 5(d)–5(f)] planes show that given an aspect ratio and an active force, a higher (lower) wrapping efficiency can be achieved under a stronger (weaker) adhesion force or a lower (higher) membrane tension, i.e., higher adhesion and looser membrane leads to faster wrapping. Such a conclusion can be supported by experimental observations [47] reported recently that higher adhesion leads to faster wrapping, and simulation results in Ref. [21] that the uptake time is strongly decreased for higher adhesion and looser membrane. All the full uptake boundaries can be very well captured by the critical conditions Eqs. (7)–(9) we obtain.

Finally, we discuss the influence of the membrane properties and the aspect ratio of particle on the wrapping process, as shown in Fig. 6. In the uptake time phase diagram in the projection of the ω-e plane for the oblate ellipsoidal particles

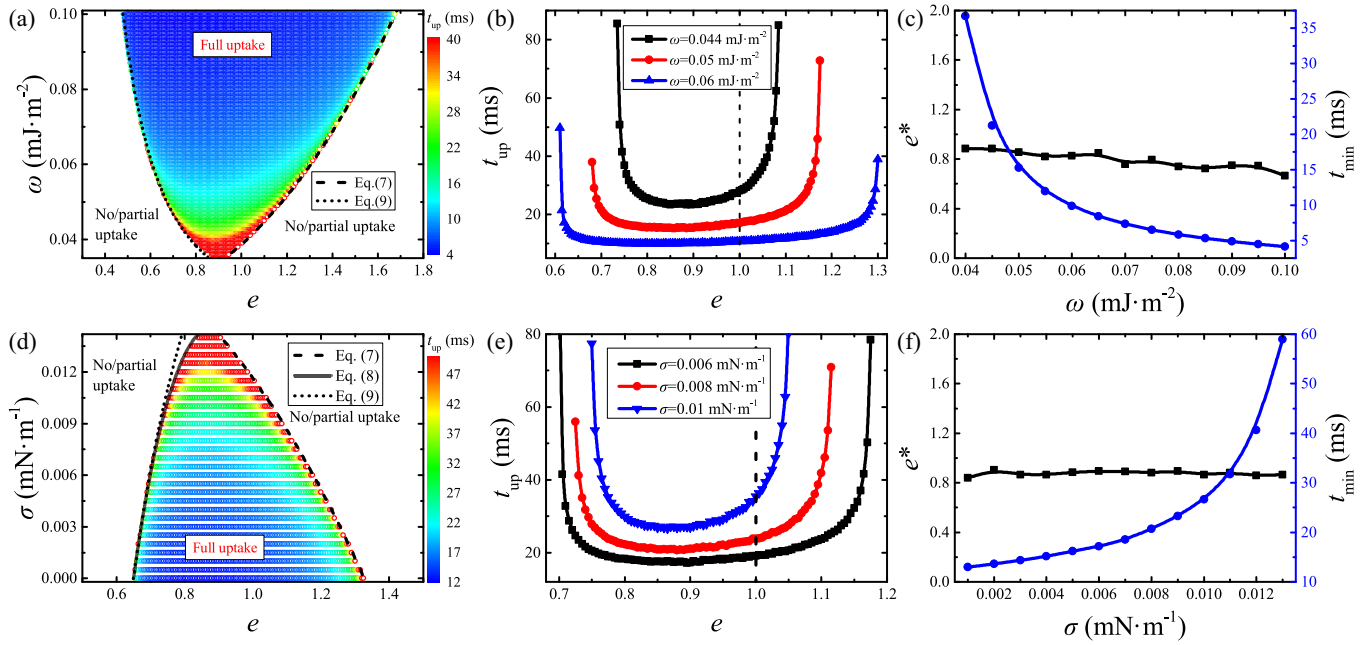

FIG. 6. Two-dimensional uptake time phase diagrams in the projection of (a) ω-e plane with how its corresponding uptake time depends on (b) aspect ratio. (c) The dependence of minimum uptake time and optimum aspect ratio on adhesion energy density. Two-dimensional uptake time phase diagrams in the projection of (d) σ-e plane with how its corresponding uptake time depends on (e) aspect ratio. (f) The dependence of minimum uptake time and optimum aspect ratio on membrane tension. The particle volume is kept fixed.

[Fig. 6(a)], the uptake time nonmonotonically depends on e, in contrast to the monotonic dependence for the prolate ellipsoidal particles [Fig. 6(b)]. The optimum aspect ratio corresponding to the minimum uptake time decreases slightly [Fig. 6(c)]. Similar analysis can be done for membrane tension [Fig. 6(d)], which comes up with similar dependence of uptake time on aspect ratio [Fig. 6(e)] but opposite dependence on membrane tension [Fig. 6(f)]. The optimum aspect ratio exhibits no response to membrane tension, like the active force. This behavior, which seems consistent with Figs. 6(a) and 6(d), comes from the mathematical feature of Eq. (6). But due to its complexity, it is still hard to get the conclusion analytically. Figure 6 also confirms that the uptake efficiency can be improved (abated) by increasing (decreasing) the adhesion energy density, or reducing (raising) the membrane tension. The dash and solid curves based on the analytical results Eqs. (7) and (8) coincide with the boundaries obtained from numerical calculations. It has been shown, by providing a stochastic model to study the kinetics of particle wrapping by a vesicle, that increasing the attraction strength between the particle and vesicle causes the improvement of uptake rate [65]. This is again a result in agreement with our present conclusions.

Consequently, we argue that the wrapping process is largely determined and controlled by the competition among the three types of energy: the elastic energy (consisting of bending energy and tension energy), the adhesive energy, and the work done by the active force. Reducing uptake time can be realized based on the condition that the adhesion energy and the work done by the active force is sufficient to overcome the energy barrier, namely, the sum of the elastic energy and the viscous dissipation. In the presence of active force, the work done by it reduces the free energy and as a result reduces the time for the full uptake to occur. According to Eq. (6), the adhesion energy driving the wrapping process is positively proportional to the adhesion energy density and negatively proportional to the membrane tension. As a result, increasing the adhesion energy density is equivalent to increasing the driving force for wrapping, and decreasing the membrane tension decreases the energy penalty for uptake, indicating a decreases of the uptake time. As for the effective dynamic viscosity, an increase means that the induced energy dissipation requires more adhesion energy and work done by the active force to compensate, which leads to an increase of uptake time.

IV. CONCLUSION

In summary, we investigate the wrapping dynamics of a nonspherical active particle by a lipid plasma membrane, by taking into account the influence of the active force, the particle shape, the effective dynamic viscosity, and the membrane properties (including the adhesion energy density and the membrane tension). The wrapping equation for the active particle is derived by using the Onsager variational principle. Two critical conditions, one for the continuous full uptake of prolate particles and the other for snapthrough full wrapping of oblate particles, are found theoretically, which precisely depict the numerical calculation results. Our results reveal that enhancing activity (active force), reducing effective dynamic viscosity, increasing adhesion energy density, and decreasing membrane tension can significantly improve the wrapping efficiency of the self-propelled nonspherical NPs. Intriguingly, with an increase of aspect ratio, the uptake time for oblate ellipsoidal particles exhibits a nonmonotonic dependence, in stark contrast to the monotonic dependence for prolate ellip-

soidal particles. These conclusions indicate that the uptake time can be manipulated by changing the activity and the aspect ratio of the particles, the effective dynamic viscosity, and the properties of the membrane, such as adhesion energy density and membrane tension. All these findings not only conclusively shed light on some previous specific investigations neglecting one or two energy contributors [2,21,48], but also give a panoramic view of the full uptake conditions for active nonspherical NPs and provide guidelines to improve the efficiency of active particle-based drug delivery systems.

ACKNOWLEDGMENTS

We acknowledge financial support from the National Natural Science Foundation of China under Grants No.12147142, No. 11974292, No. 12174323, and No. 1200040838, and 111 project B16029.

APPENDIX: DERIVATION OF EQS. (2)–(4)

In practice, the mean curvature of the ellipsoidal particle is given by

$$H = \frac{c_1 + c_2}{2} = \frac{b[2a^2 + (b^2 - a^2)\sin^2\theta]}{2a[a^2 + (b^2 - a^2)\sin^2\theta]^{3/2}}, \tag{A1}$$

where c_1 and c_2 are the two principle curvatures. Substituting the area element and Eq. (A1) into the first term of Eq. (1) and using $e = b/a$, one can obtain Eq. (2). In Eq. (1), ΔA is the excess area, which equals the area difference between the contact area and the area of its projection. As a result, the excess area can be calculated as

$$\Delta A = \int_0^{\alpha} \left(1 - \frac{a\cos\theta}{\sqrt{a^2\cos^2\theta + b^2\sin\theta}}\right) dA. \tag{A2}$$

Substituting Eq. (A2) into the second term of Eq. (1) and using $e = b/a$, one can obtain Eq. (3). During the uptake process, the friction force per unit length near the membrane-particle contact line is given by $f_{\text{friction}} = \eta\sqrt{a^2\cos^2\alpha + b^2\sin\alpha}\dot{\alpha}$. Then the total friction force at the contact line reads $F_{\text{friction}} = L(\alpha) f_{\text{friction}}$. In the case of low Reynolds number, the dissipation function is given by

$$\Phi = \tfrac{1}{2} F_{\text{friction}} \sqrt{a^2\cos^2\alpha + b^2\sin\alpha}\dot{\alpha}. \tag{A3}$$

A simplification of the above equation leads to Eq. (4).

[1] B. Alberts, *Molecular Biology of the Cell* (Garland Science, New York, 2015).
[2] F. Frey, F. Ziebert, and U. S. Schwarz, Phys. Rev. E **100**, 052403 (2019).
[3] G. V. Meer and H. Sprong, Curr. Opin. Cell Biol. **16**, 373 (2004).
[4] J. T. Groves and J. Kuriyan, Nat. Struct. Mol. Biol. **17**, 659 (2010).
[5] G. Bao and X. R. Bao, Proc. Natl. Acad. Sci. USA **102**, 9997 (2005).
[6] S. Zhang, H. Gao, and G. Bao, ACS Nano **9**, 8655 (2015).
[7] S. Behzadi, V. Serpooshan, W. Tao, M. A. Hamaly, M. Y. Alkawareek, E. C. Dreaden, D. Brown, A. M. Alkilany, O. C. Farokhzad, and M. Mahmoudi, Chem. Soc. Rev. **46**, 4218 (2017).
[8] D. Peer, J. M. Karp, S. Hong, O. C. Farokhzad, R. Margalit, and R. Langer, Nat. Nanotechnol. **2**, 751 (2007).
[9] W. Rao, H. Wang, J. Han, S. Zhao, J. Dumbleton, P. Agarwal, W. Zhang, G. Zhao, J. Yu, D. L. Zynger, X. Lu, and X. He, ACS Nano **9**, 5725 (2015).
[10] Y. Min, J. M. Caster, M. J. Eblan, and A. Z. Wang, Chem. Rev. **115**, 11147 (2015).
[11] N. Kol, Y. Shi, M. Tsvitov, D. Barlam, R. Z. Shneck, M. S. Kay, and I. Rousso, Biophys. J. **92**, 1777 (2007).
[12] R. F. Bruinsma, G. J. L. Wuite, and W. H. Roos, Nat. Rev. Phys. **3**, 76 (2021).
[13] C. B. Jackson, M. Farzan, B. Chen, and H. Choe, Nat. Rev. Mol. Cell Bio. **23**, 3 (2022).
[14] M. Deserno and W. M. Gelbart, J. Phys. Chem. B **106**, 5543 (2002).
[15] M. Deserno and T. Bickel, Europhys. Lett. **62**, 767 (2003).
[16] M. Deserno, Phys. Rev. E **69**, 031903 (2004).
[17] S. Zhang, J. Li, G. Lykotrafitis, G. Bao, and S. Suresh, Adv. Mater. **21**, 419 (2009).
[18] B. D. Chithrani, A. A. Ghazani, and W. C. W. Chan, Nano Lett. **6**, 662 (2006).
[19] J. Agudo-Canalejo and R. Lipowsky, ACS Nano **9**, 3704 (2015).
[20] C. Contini, J. W. Hindley, T. J. Macdonald, J. D. Barritt, O. Ces, and N. Quirke, Commun. Chem. **3**, 130 (2020).
[21] F. Frey, F. Ziebert, and U. S. Schwarz, Phys. Rev. Lett. **122**, 088102 (2019).
[22] K. Yang and Y. Ma, Nat. Nanotechnol. **5**, 579 (2010).
[23] Z. Shen, H. Ye, X. Yi, and Y. Li, ACS Nano **13**, 215 (2019).
[24] X. Yi, X. Shi, and H. Gao, Phys. Rev. Lett. **107**, 098101 (2011).
[25] J. C. Shillcock and R. Lipowsky, Nat. Mater. **4**, 225 (2005).
[26] X. Yi and H. Gao, Phys. Rev. E **89**, 062712 (2014).
[27] A. Verma and F. Stellacci, Small **6**, 12 (2010).
[28] X. Ma, X. Yang, M. Li, J. Cui, P. Zhang, Q. Yu, and J. Hao, Langmuir **37**, 11688 (2021).
[29] H. Yuan, J. Li, G. Bao, and S. Zhang, Phys. Rev. Lett. **105**, 138101 (2010).
[30] H. Yuan and S. Zhang, Appl. Phys. Lett. **96**, 033704 (2010).
[31] T. Wiegand, M. Fratini, F. Frey, K. Yserentant, Y. Liu, E. Weber, K. Galior, J. Ohmes, F. Braun, D.-P. Herten, S. Boulant, U. S. Schwarz, K. Salaita, E. A. Cavalcanti-Adam, and J. P. Spatz, Nat. Commun. **11**, 32 (2020).
[32] J. Agudo-Canalejo and R. Lipowsky, Nano Lett. **15**, 7168 (2015).
[33] H. T. Spanke, R. W. Style, C. François-Martin, M. Feofilova, M. Eisentraut, H. Kress, J. Agudo-Canalejo, and E. R. Dufresne, Phys. Rev. Lett. **125**, 198102 (2020).
[34] P. M. Colonne, C. G. Winchell, and D. E. Voth, Front. Cell. Infect. Microbiol. **6**, 107 (2016).

[35] J. A. Theriot, T. J. Mitchison, L. G. Tilney, and D. A. Portnoy, Nature (London) **357**, 257 (1992).
[36] J. R. Robbins, A. I. Barth, H. Marquis, E. L. de Hostos, W. J. Nelson, and J. A. Theriot, J. Cell Biol. **146**, 1333 (1999).
[37] T. Chakraborty, Immunobiology **201**, 155 (1999).
[38] F. E. Ortega, E. F. Koslover, and J. A. Theriot, eLife **8**, e40032 (2019).
[39] G. C. Dowd, R. Mortuza, M. Bhalla, H. V. Ngo, Y. Li, L. A. Rigano, and K. Ireton, Proc. Natl. Acad. Sci. USA **117**, 3789 (2020).
[40] H. R. Vutukuri, M. Hoore, C. Abaurrea-Velasco, L. van Buren, A. Dutto, T. Auth, D. A. Fedosov, G. Gompper, and J. Vermant, Nature (London) **586**, 52 (2020).
[41] S. C. Takatori and A. Sahu, Phys. Rev. Lett. **124**, 158102 (2020).
[42] C. Wang, Y.-K. Guo, W.-D. Tian, and K. Chen, J. Chem. Phys. **150**, 044907 (2019).
[43] Y. Li and P. R. ten Wolde, Phys. Rev. Lett. **123**, 148003 (2019).
[44] M. S. E. Peterson, A. Baskaran, and M. F. Hagan, Nat. Commun. **12**, 7247 (2021).
[45] L. Le Nagarda, A. T. Browna, A. Dawsona, V. A. Martineza, W. C. K. Poona, and M. Staykova, Proc. Natl. Acad. Sci. USA **119**, e2206096119 (2022).
[46] A. T. Brown, I. D. Vladescu, A. Dawson, T. Vissers, J. Schwarz-Linek, J. S. Lintuvuori, and W. C. K. Poon, Soft Matter **12**, 131 (2016).
[47] H. T. Spanke, J. Agudo-Canalejo, D. Tran, R. W. Style, and E. R. Dufresne, Phys. Rev. Res. **4**, 023080 (2022).
[48] P. Chen, Z. Xu, G. Zhu, X. Dai, and L.-T. Yan, Phys. Rev. Lett. **124**, 198102 (2020).
[49] J. Panyam and V. Labhasetwar, Adv. Drug Delivery Rev. **55**, 329 (2003).
[50] X. Xu, S. Hou, N. Wattanatorn, F. Wang, Q. Yang, C. Zhao, X. Yu, H.-R. Tseng, S. J. Jonas, and P. S. Weiss, ACS Nano **12**, 4503 (2018).
[51] W. Wang, Z. Wu, X. Lin, T. Si, and Q. He, J. Am. Chem. Soc. **141**, 6601 (2019).
[52] M. Medina-Sánchez, V. Magdanz, M. Guix, V. M. Fomin, and O. G. Schmidt, Adv. Funct. Mater. **28**, 1707228 (2018).
[53] H. Xie, M. Sun, X. Fan, Z. Lin, W. Chen, L. Wang, L. Dong, and Q. He, Sci. Robot. **4**, eaav8006 (2019).
[54] R. Weissleder, Science **312**, 1168 (2006).
[55] C. Hulo, E. De Castro, P. Masson, L. Bougueleret, A. Bairoch, I. Xenarios, and P. Le Mercier, Nucleic Acids Res. **39**, D576 (2011).
[56] S. Dasgupta, T. Auth, N. S. Gov, T. J. Satchwell, E. Hanssen, E. S. Zuccala, D. T. Riglar, A. M. Toye, T. Betz, J. Baum, and G. Gompper, Biophys. J. **107**, 43 (2014).
[57] L. P. Chen, S. Y. Xiao, H. Zhu, L. Wang, and H. J. Liang, Soft Matter **12**, 2632 (2016).
[58] W. Helfrich, Z. Naturforsch. C **28**, 693 (1973).
[59] F. Jülicher and U. Seifert, Phys. Rev. E **49**, 4728 (1994).
[60] L. Onsager, Phys. Rev. **37**, 405 (1931).
[61] L. Onsager, Phys. Rev. **38**, 2265 (1931).
[62] L. Foret, Eur. Phys. J. E **37**, 42 (2014).
[63] G. Kumar and A. Sain, Phys. Rev. E **94**, 062404 (2016).
[64] A. Khosravanizadeh, P. Sens, and F. Mohammad-Rafiee, J. R. Soc. Interface **19**, 20220462 (2022).
[65] S. Mirigian and M. Muthukumar, J. Chem. Phys. **139**, 044908 (2013).